Crystal fields in $YbInNi_4$ determined with magnetic form factor and inelastic neutron scattering

A. Severing,[1] F. Givord,[2] J.-X. Boucherle,[2] T. Willers,[1] M. Rotter,[3] Z. Fisk,[4] A. Bianchi,[5] M. T. Fernandez-Diaz,[6] A. Stunault,[6] B. D. Rainford,[7] J. Taylor,[8] and E. Goremychkin[8]

[1]*Institute of Physics II, University of Cologne, Zülpicher Straße 77, D-50937 Cologne, Germany*

[2]*CEA-Grenoble, DSM/DRFMC/SPSMS/MDN, F-38054 Grenoble Cedex 9, France*

[3]*Max Planck Institute CPfS, Nöthnizer Straße 40, D-01187 Dresden, Germany*

[4]*University of California, Irvine, California, USA*

[5]*Département de Physique and Regroupement Québécois sur les Matériaux de Pointe, Université de Montréal, Montréal, Quebec H3C 3J7, Canada*

[6]*Institut Laue Langevin, 6 rue Horowitz, F-38042 Grenoble, France*

[7]*School of Physics and Astronomy, University of Southampton, Southampton SO17 1BJ, United Kingdom*

[8]*ISIS Facility, Rutherford Appleton Laboratory, Chilton, Didcot, Oxfordshire OV11 0QX, United Kingdom*

(Received 17 December 2010; published 14 April 2011)

The magnetic form factor of $YbInNi_4$ has been determined via the flipping ratios R with polarized neutron diffraction, and the scattering function $S(Q,\omega)$ was measured in an inelastic neutron scattering experiment. Both experiments were performed with the aim of determining the crystal-field scheme. The magnetic form factor clearly excludes the possibility of a Γ_7 doublet as the ground state. The inelastic neutron data exhibit two almost equally strong peaks at 3.2 meV and 4.4 meV which points, in agreement with earlier neutron data, toward a Γ_8 quartet ground state. Further possibilities such as a quasiquartet ground state are discussed.

DOI: 10.1103/PhysRevB.83.155112 PACS number(s): 71.27.+a, 75.10.Dg, 78.70.Nx, 75.30.Mb

I. INTRODUCTION

$YbInNi_4$ came into the focus of interest when the first-order valence transition from a trivalent high-temperature to an intermediate low-temperature phase was discovered in $YbInCu_4$.[1] In many rare-earth compounds the $4f$ electrons couple with the conduction electrons, leading to a wealth of properties from magnetic order, to Kondo and heavy-fermion states with nonconventional superconductivity and/or non-Fermi liquid behavior, and to intermediate valency. Hence the knowledge of the low-energy excitations, especially the ground-state wave function of the $4f$ electrons involved, is crucial for any further understanding of what mechanism leads to what property. The crystal-field splitting of $YbInCu_4$ is difficult to study directly because of its intermediate valent state at low temperatures. Instead $YbInNi_4$ has been investigated, because it is trivalent over the entire temperature range. However, there are many discrepancies between the different crystal-field proposals,[2–5] so we reinvestigated the crystal-field scheme of $YbInNi_4$ with polarized neutron diffraction and inelastic neutron scattering.

At high temperatures $YbInNi_4$ shows Curie-Weiss behavior with the full Yb^{3+} magnetic moment and orders magnetically at 3 K.[2] $YbInNi_4$ forms in the cubic C15b Laves structure with T_d symmetry at the Yb site, so that the eightfold degenerate Hund's rule ground state of Yb^{3+} with $J = 7/2$ and $J_z = |\pm 7/2\rangle, |\pm 5/2\rangle, |\pm 3/2\rangle, |\pm 1/2\rangle$ is lifted by the crystal-field into two Kramers doublets $|\Gamma_6\rangle$ and $|\Gamma_7\rangle$, and one quartet $|\Gamma_8\rangle$. In cubic site symmetry the J_z admixture of these crystal-field wave functions is fixed so that the crystal-field scheme is fully determined with the crystal-field transition energies and the sequence of states. In the Stevens approximation the transition energies and sequence of states are given by the Stevens parameters. For Yb^{3+} with cubic T_d symmetry the two Stevens parameters B_4^0 and B_6^0 fully describe the crystal-field scheme.[6]

There has been a controversy about the crystal-field schemes for several years and they became of interest again because of the more recent discovery that applying pressure (2.45 GPa) to $YbInCu_4$ suppresses the valence transition and leads to magnetic order at 2.4 K.[7–9] There are several crystal-field propositions which are briefly summarized in the following: (1) Inelastic neutron scattering data by Severing *et al.*[3] showed a double peak structure at low temperatures and the excitations at about 3 and 4 meV were interpreted as transitions from a quartet ground state because the transition matrix element between the two doublets is zero.[10] (2) Sarrao *et al.* concluded from their entropy findings in the specific heat that the ground state should be a doublet and they specified from magnetization data that it should be the $|\Gamma_7\rangle$ state. Best fits were obtained when assuming the second doublet at 5.5 meV and the $|\Gamma_8\rangle$ quartet at 10.5 meV.[2] (3) From rare-earth-doped $LuInNi_4$ data of the magnetic susceptibility and from ESR measurements Pagliuso *et al.* suggest also a $|\Gamma_7\rangle$ ground state with the $|\Gamma_8\rangle$ quartet at 4 meV and the $|\Gamma_6\rangle$ doublet at 9 meV.[4] (4) Aviani *et al.* and Park *et al.* investigated the crystal-field ground state of $YbInCu_4$, where Aviani *et al.* suppressed the valence transition with 50% Y doping and Park *et al.* by applying pressure. Aviani *et al* describe their specific heat data well with a quasiquartet ground state which is the inverse of the scheme of Severing *et al.*, while Park *et al.* describe their specific heat data under pressure best with the $|\Gamma_8\rangle$ quartet scenario and a total splitting of 28 K when taking the Kondo effect into account,[5,11] which is in agreement with the neutron proposal for $YbInNi_4$.

II. EXPERIMENTAL AND ANALYSIS

These different proposition challenged us to make another attempt to determine the crystal-field scheme of $YbInNi_4$ with neutron scattering. We have measured the low-temperature magnetic form factor, which probes directly the ground-state

TABLE I. Values of the indium scattering length (real part b_{In} and imaginary part b''_{In}) and of the total absorption coefficient $\mu_{\mathrm{YbInNi_4}}$ as a function of the wavelength λ.

Device	λ (Å)	b_{In} (fm)	b''_{In} (fm)	$\mu_{\mathrm{YbInNi_4}}$ (cm^{-1})
D9	0.84	0.3924	−0.0060	1.42
	0.51	0.3537	−0.0083	1.21
D3	0.825	0.3917	−0.0061	1.42
	0.74	0.3867	−0.0063	1.34
	0.52	0.3564	−0.0081	1.21

wave function as a Fourier transform of the spatial distribution of the 4*f* electron moment; i.e., it is directly sensitive to the anisotropy of the crystal-field ground state. Moreover, we have performed inelastic neutron scattering experiments on a powder sample with emphasis on measuring excitations at low temperatures with a resolution better than that in Ref. 3. Crystals were grown by flux growth and the C15b structure has been verified by powder x-ray diffraction.

A. Magnetic form factor

The magnetic scattering intensity in an elastic neutron scattering experiment is determined by the magnetic structure factor F_M where

$$F_M = \frac{r_0}{2\mu_B} \sum_n |\mathbf{m}_n|(\mathbf{Q}) \exp(i\mathbf{Q}\mathbf{R}_n) \exp(-W_n) \qquad (1)$$

and where $\mathbf{m}(\mathbf{Q})$ is the Fourier transform of the magnetization density at the scattering vector $\mathbf{Q}$. The summation is over the n atoms of the magnetic unit cell, $\exp(-W_n)$ is the Debye-Waller factor and R_n the position of the nth atom, μ_B is the Bohr magneton, and $r_0 = \gamma \frac{e^2}{mc^2}$ with $\gamma = -1.92$ the gyromagnetic ratio of the neutron. In the dipole approximation $\mathbf{m}(\mathbf{Q})$ depends only on $|\mathbf{Q}|$ and can be written as the product of the magnetic moment $\mathbf{m}$ and the spherical magnetic form factor $f(|\mathbf{Q}|)$, $\mathbf{m}(|\mathbf{Q}|) = \mathbf{m} f(|\mathbf{Q}|)$. $f(|\mathbf{Q}|)$ is listed in text books.[12] However, the dipole approximation is not valid for large momentum transfers and/or when the spatial distribution of magnetic moments is strongly anisotropic as for $4f$ moments in the presence of a crystal field. Then the magnetic scattering intensity is proportional to $|\mathbf{m}_\perp(\mathbf{Q})|^2$, which is the square of the projection of $\mathbf{m}(\mathbf{Q})$ perpendicular to $\mathbf{Q}$. This introduces in addition to the modulus a *vector* $\mathbf{Q}$ dependence to the magnetic intensities which does not exist in the dipole approximation. This vector $\mathbf{Q}$ dependence of $\mathbf{m}_\perp(\mathbf{Q})$ can be used to determine crystal-field ground-state wave functions (see, e.g., Refs. 13–15). Here we determined the vector $\mathbf{Q}$ dependence of $\mathbf{m}(\mathbf{Q})$ of Yb^{3+} with the aim of obtaining the ground-state wave function of $YbInNi_4$. A polarized neutron diffraction experiment was performed on a $YbInNi_4$ single crystal using the D3 diffractometer at the high-flux reactor of the Institut Laue-Langevin in Grenoble. The peak intensity of the Bragg reflections, which is measured for neutrons polarized parallel and antiparallel to the applied magnetic field, leads to the so-called flipping ratio $R = I^+/I^-$. To deduce the magnetic contribution from R, a good knowledge of the nuclear structure factors F_N is necessary. This was achieved by an experiment on the same crystal on the 4-circle diffractometer D9 at ILL.

The nuclear intensity measurements with unpolarized neutrons (D9) were performed at $T = 5$ K with two different wavelengths $\lambda = 0.84$ Å (1146 Bragg reflections) and $\lambda = 0.51$ Å (698 Bragg reflections). The crystal structure of our sample was refined to the C15b structure with the program MXD.[16] The scattering lengths were taken from the BNL tables[17] as 12.43 fm for ytterbium and 10.3 fm for nickel. As the scattering length of indium depends strongly on the wavelength, its real and imaginary parts (b and b'', respectively) were calculated for each wavelength from the values given at 1.8 Å. The total absorption coefficient μ was also calculated and all these wavelength-dependent values are gathered in Table I. The nickel atomic position x_{Ni}, the Debye-Waller thermal parameters W_n, and the extinction parameters, block size t, and mosaicity g[18] were refined, leading to consistent values at both wavelengths. These values are given in Table II.

The polarized neutron diffraction experiments (D3) were performed at two temperatures, 5 and 20 K, in a field of $H = 2$ T applied along the $[1\bar{1}0]$ axis of the crystal. The selected wavelength was $\lambda = 0.825$ Å, and two erbium filters were used to suppress the $\lambda/2$ contamination. To optimize the extinction corrections,[19,20] flipping ratios of some particular reflections

TABLE II. Results of the refinements of the nuclear structure. Values of the nickel atomic position x_{Ni}, the Debye-Waller thermal parameters W_n, extinction parameters t and g, and $\chi^2 = \sum_i p_i (A_i^{\mathrm{obs}} - A_i^{\mathrm{calc}})^2/(N_{\mathrm{obs}} - N_{\mathrm{var}})$ with $p_i = 1/\sigma^2$ and $A_i = I_i$ (intensity) for D9 or $A_i = R_i$ (flipping ratio) for D3.

Device	λ (Å)	x_{Ni}	W_{Yb} (Å^2)	W_{In} (Å^2)	W_{Ni} (Å^2)	t (μm)	g (10^{-4} rad^{-1})	χ^2
D9 refined	0.84	0.625 73 (±0.000 02)	0.083 (±0.006)	0.178 (±0.011)	0.140 (±0.005)	4.8 (±0.7)	0.074 (±0.006)	
	0.51	0.625 83 (±0.000 04)	0.146 (±0.016)	0.113 (±0.033)	0.179 (±0.014)	5.2 (±2.6)	0.094 (±0.023)	4.5
D3 refined	3λ	0.625 75	0.10	0.15	0.15	5.0	0.094 (±0.013)	2.4
D3 final	3λ	0.625 75 (±0.000 05)	0.10 (±0.03)	0.15 (±0.03)	0.15 (±0.03)	5.0	0.09 (±0.02)	

were also measured at two lower wavelengths $\lambda = 0.74$ Å and $\lambda = 0.52$ Å, thus taking advantage of the hot source available on D3.

In $YbInNi_4$, the nuclear and magnetic structure factors are complex. Their imaginary part has two origins: The imaginary scattering length of indium and the non-centrosymmetric structure of $YbInNi_4$. This second feature affects the ytterbium contribution to the structure factor only for Bragg reflections with h,k,l odd since the Yb occupy the $4c$ lattice sites at $\frac{1}{4}\frac{1}{4}\frac{1}{4}$. Note that the expectation value $\mathbf{m}_\perp(\mathbf{Q})$ is real for any $4f$ wave function, so that the magnetic structure factor F_M is real for h,k,l even. For $\mathbf{m}(\mathbf{Q}) \parallel \mathbf{H}$ the flipping ratio R can then be written (see, e.g., Ref. 21)

$$R = \frac{F_N'^2 + F_N''^2 + 2\sin^2\alpha F_N' F_M + \sin^2\alpha F_M^2}{F_N'^2 + F_N''^2 - 2\sin^2\alpha F_N' F_M + \sin^2\alpha F_M^2}. \qquad (2)$$

F_N' and F_N'' are the real and imaginary parts of the nuclear structure factor F_N and α is the angle between the magnetic moment $\mathbf{m}(\mathbf{Q})$ and the scattering vector $\mathbf{Q}$. This formula undergoes appropriate corrections in order to take into account instrumental imperfections (polarization of the incident beam, flipping efficiency) and extinction effects.

Fifty-five nonequivalent reflections were measured at $T = 5$ K and 49 at $T = 20$ K, up to $\sin\theta/\lambda = 0.94$Å^{-1}. Among them, 13 independent reflections measured at several different wavelengths were used to refine the extinction parameters. With fixing the Ni positions x_{Ni}, the Debye Waller parameters W_n, and block size t to the values deduced from the refinements on D9, the mosaicity g was refined to a value in complete agreement with the previous ones (see Table II). The final values of the different parameters used for the data analysis are also given in Table II (see Ref. 19,20).

The F_M values deduced from the measured flipping ratios are directly related to the Fourier transform of the magnetization density $\mathbf{m}(\mathbf{Q})$ for the scattering vector $\mathbf{Q}$ [see Eq. (1)]. Figure 1 shows the obtained $|\mathbf{m}(\mathbf{Q})|$ values at 5 K and 20 K versus $\sin\theta/\lambda$ with $|\mathbf{Q}|=4\pi\sin\theta/\lambda$. At 5 K there is an anisotropy; i.e., all Bragg reflections lie between the $(hh0)$ and the $(00l)$ type ones. The $(00l)$ reflections decrease steeper

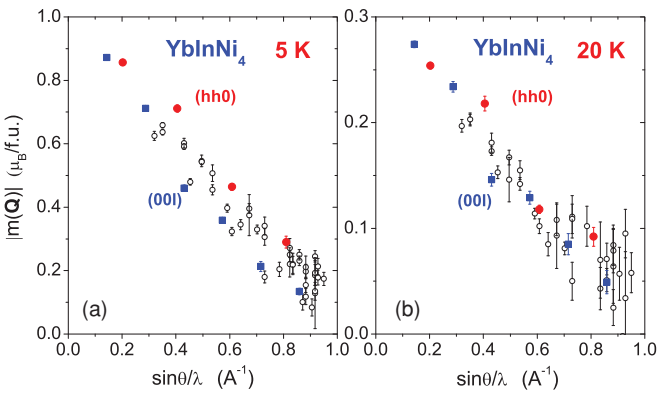

FIG. 1. (Color online) Ytterbium magnetic amplitudes $|\mathbf{m}(\mathbf{Q})|$ measured with an applied field of 2 T at $T = 5$ K (a) and $T = 20$ K (b). The full blue squares correspond to (00l), the full red circles to (hh0), and the black open squares to other reflections with even indices.

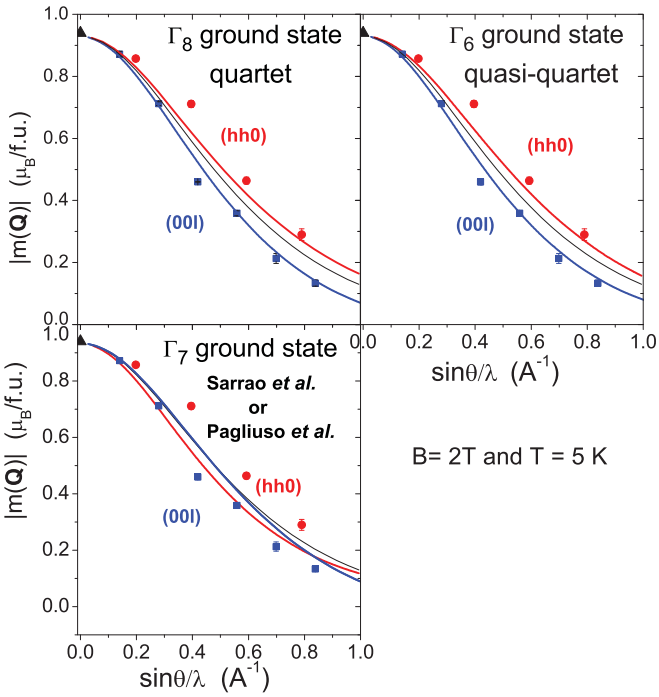

FIG. 2. (Color online) Comparison of simulated ytterbium magnetic amplitudes $|\mathbf{m}(\mathbf{Q})|$ at $T = 5$ K for different ground states. The full symbols are the measured values for $(00l)$ (blue squares) and $(hh0)$ (red circles); the lines are simulations for the $(00l)$ (blue) and $(hh0)$ (red) directions for the different crystal-field propositions. The black line corresponds to the spherical form factor. The values for $\sin\theta/\lambda = 0$ (black triangles) come from magnetization.

with $\sin\theta/\lambda$ than the $(hh0)$ ones. At 20 K, this anisotropy has nearly vanished.

Only these special reflections are drawn in Fig. 2. We have now simulated $|\mathbf{m}(\mathbf{Q})|$ for the different crystal-field scenarios as suggested in Refs. 2–5. The simulation was performed with the program package McPhase[22] which includes form factor calculations beyond dipole approximation. Figure 2 displays the measured $|\mathbf{m}(\mathbf{Q})|$ values for the $(00l)$ and $(hh0)$ reflections as full symbols. The value for $\sin\theta/\lambda = 0$ is taken from magnetization. The solid lines are simulations. For the current plot the simulations have been scaled to the value at $\sin\theta/\lambda = 0$. The scaling factors are 1.07, 1.05, and 0.95 for the $|\Gamma_6\rangle$, $|\Gamma_7\rangle$, and $|\Gamma_8\rangle$ simulation. The simulations show that a $|\Gamma_7\rangle$ ground state would yield the wrong anisotropy: For a $|\Gamma_7\rangle$ the $(hh0)$ reflections decrease steeper with $\sin\theta/\lambda$ than the $(00l)$ which is in contradiction to our observation. Hence our form factor measurements clearly rule out the possibility of $|\Gamma_7\rangle$ as ground state. In contrast, the simulations for the $|\Gamma_6\rangle$ ground state of the quasiquartet scenario and the for the $|\Gamma_8\rangle$ quartet both give the correct anisotropy.

B. Inelastic neutron scattering

Inelastic neutron scattering experiments on polycrystalline samples are the most common technique to determine crystal-field excitations in rare-earth compounds. Here we present inelastic neutron data of polycrystalline $YbInNi_4$ which were taken at the time-of-flight spectrometer MARI at the pulsed neutron source ISIS with an incident energy of 12 meV

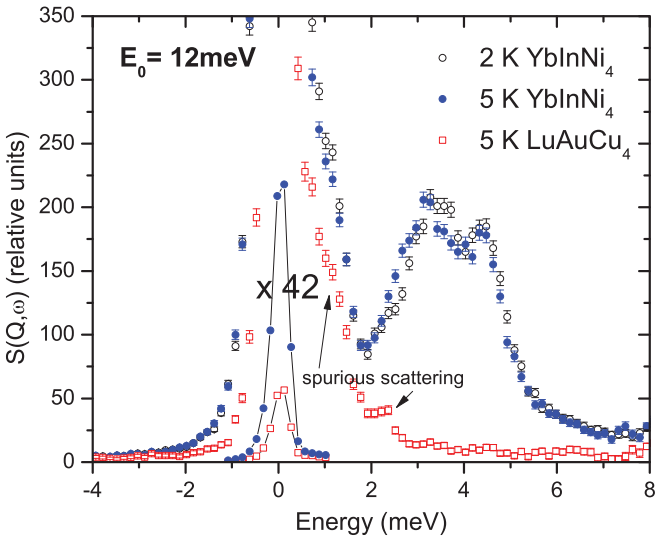

FIG. 3. (Color online) Scattering function of $YbInNi_4$ for $|\mathbf{Q}|$ in between 0.35 Å^{-1} and 2.3 Å^{-1} at 2 K (open black circles) and 5 K (full blue circles), and of $LuAuCu_4$ (open red squares), also at 5 K. The insets represent the elastic scattering divided by 42. The extra scattering in the $YbInN_4$ data between 2.5 meV and 6 meV is attributed to magnetic scattering.

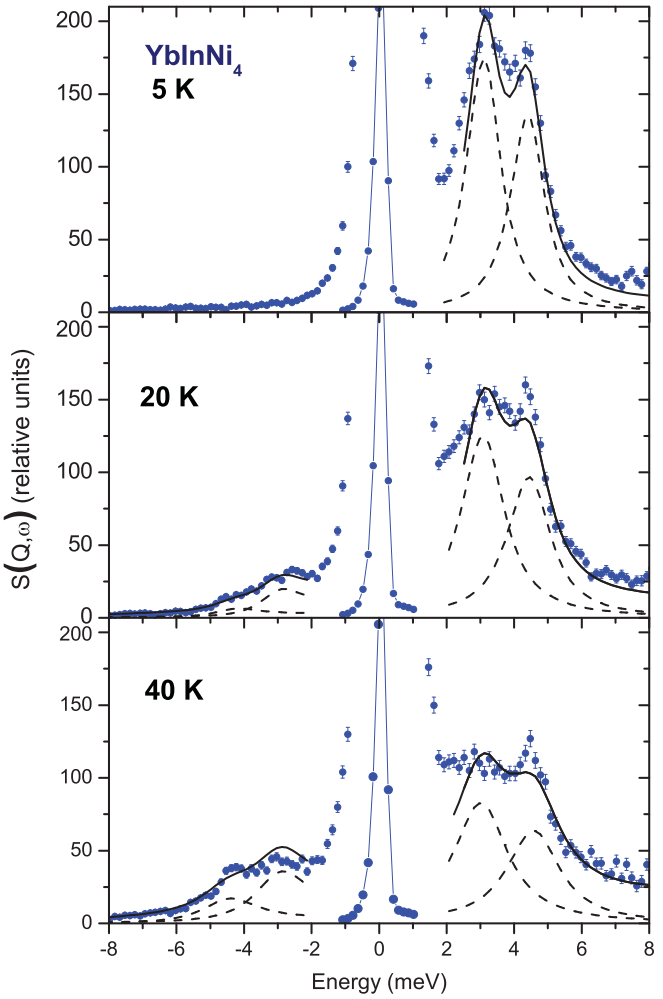

FIG. 4. (Color online) Temperature evolution of the scattering function of $YbInNi_4$ for 12 meV incident energy and $|\mathbf{Q}|$ in between 0.35 Å^{-1} and 2.3 Å^{-1}. The insets represent the elastic scattering divided by 42, the dashed lines show crystal-field excitations resulting from a crystal-field fit, and the solid lines are the total fitted magnetic scattering. Note, the fitting region was restricted to energy transfers below −2 meV and above 2.5 meV to avoid the strong elastic and the spurious scattering at the tail of the elastic line.

and a resolution of 0.4 meV (FWHM) at elastic scattering. Detectors from $2\theta = 8^\circ$ to 52° are grouped together, resulting in an averaged Q vector at elastic scattering of 1.34 Å. The sample was mounted in a cryostat and data were taken in the magnetically ordered phase at 2 K and in the paramagnetic phase at 5 K, 20 K, and 40 K.

Figure 3 shows the scattering function $S(Q,\omega)$ versus energy transfer for $YbInNi_4$ at 2 and 5 K, and of the nonmagnetic isostructural compound $LuAuCu_4$, also at 5 K. The data are corrected for detector efficiency and absorption, and are scaled to sample mass so that the scattering intensities are comparable. Due to the smaller nuclear cross section of $LuAuCu_4$ with respect to $YbInNi_4$ the elastic scattering of the latter is stronger. The Lu data prove that phonon scattering is negligible in the present energy window and detector grouping. The extra scattering of the $YbInNi_4$ sample between 2.5 meV and 6 meV is therefore identified as magnetic scattering. The shoulder which appears on the neutron energy loss side of the elastic line appears in the spectra of the magnetic and nonmagnetic sample, and is attributed to spurious Bragg scattering in either sample which has been reflected from the cryostat walls, reaching the detectors time delayed, and therefore in an inelastic channel. Since it is difficult to account for this quantitatively and since we know from previous high-resolution data[3] that the quasielastic scattering of $YbInNi_4$ is too narrow to be resolved in the present experiment we concentrate on the inelastic scattering above 2.5 meV and on the neutron energy gain side for $T = 20$ K and 40 K.

The magnetic scattering intensity between 2.5 meV and 6 meV consists clearly of two lines. At 5 K these lines can be fitted with two Lorentzians centered at about 3.2 ± 0.1 meV and 4.4 ± 0.1 meV. In the magnetically ordered phase at 2 K the lower crystal-field excitation appears at slightly larger energy transfers with respect to 5 K which is probably due to the influence of the magnetic order at 2 K. The linewidths remain unchanged.

Figure 4 shows the temperature evolution of the scattering function in the paramagnetic phase from 5 K, 20 K to 40 K. The double peak structure survives up to 40 K without a shift in energy, although the excitations become broader as temperature rises. The present incoming neutron energy of 12 meV provides an energy window up to 10 meV. At none of the temperatures magnetic scattering was detected at energy transfers larger than than 4.4 meV.

The scattering function $S(Q,\omega)$ can exhibit two magnetic excitations at 2 and 5 K only if

(a) the ground state is the $|\Gamma_8\rangle$ quartet and two ground-state excitations into the $|\Gamma_6\rangle$ and $|\Gamma_7\rangle$ doublets take place, or

(b) the ground state is a quasiquartet and the two doublets which are 1 meV apart are sufficiently populated, or

(c) the crystal-field states are Zeeman split due to the proximity of the magnetically ordered state—then even a doublet could give rise to two ground-state excitations—or

(d) some structural distortion is present, so that the site symmetry is no longer cubic.

Proposition (a) is based on the fact that the transition matrix element between the two doublets is zero.[10] This new set of data is also, like the previously reported neutron data, well described with a $|\Gamma_8\rangle$ quartet ground state. For a quantitative analysis the magnetic form factor has to be taken into account. Here, for the purpose of describing nondispersive excitations in a powder sample, it is sufficient to use the spherical, textbook magnetic form factor $f(|\mathbf{Q}|)$.[12] The result of a quantitative crystal-field analysis where all three temperatures were fitted simultaneously is shown in Fig. 4 (see black lines). For both excitations the same linewidth was assumed. The fitted line widths increase with temperature from 0.54 ± 0.05 meV at 5 K to 0.7 ± 0.05 meV at 20 K and 0.9 ± 0.08 meV at 40 K. The best fit was obtained for $B_4^0 = -1.110^{-3}$ meV and $B_6^0 = -8.8810^{-5}$ meV, which is consistent with Ref. 3 but seemingly in conflict with the entropy findings of the specific heat[2]. Although (b), the quasiquartet scenario *à* la Aviani *et al.*,[5] is tempting, a simple simulation of the scattering function for a quasiquartet ground state excludes this possibility as an explanation for the inelastic neutron data of $YbInNi_4$: Neither at 2 nor at 5 K is the first excited doublet at 1 meV sufficiently populated to give rise to two almost equally strong excitations. This is demonstrated in Fig. 5 where the result of a crystal-field simulation with a quasiquartet ground state is shown for 5 K. Possibility (c) of a molecular field split doublet ground state could give rise to two excitations at low temperatures, but for, e.g., a $|\Gamma_6\rangle$ ground state the same molecular field of $\approx$0.33 meV would have to be assumed for the magnetically ordered and the paramagnetic phase. Another difficulty with this assumption is that at higher temperatures, when no Zeeman splitting and intermixing of states due to a molecular field is present, the spectra should be shifted in energy with respect to the low-temperature data. This has not been observed. Possibility (d) of a structural distortion can be ruled out from our structural analysis which is part of the form factor measurement and from x-ray data which were taken in order to verify sample quality. Hence, this new set of neutron data confirms the previous inelastic neutron scattering results of a $|\Gamma_8\rangle$ quartet ground state.

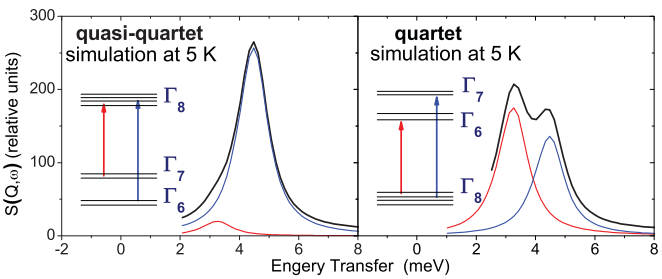

FIG. 5. (Color online) Simulated inelastic scattering function at 5 K for a quasiquartet (left) and quartet (right) ground-state crystal-field model.

III. DISCUSSION

The observed anisotropy of the magnetic form factor is clearly not compatible with the spatial distribution of a $|\Gamma_7\rangle$ ground state although magnetization and susceptibility measurements[2,4] favor $|\Gamma_7\rangle$. We believe that the information obtained from a form factor experiment is more robust for the following reasons: The magnetic form factor when measured on a single crystal probes directly the orbital shape of the lowest Zeeman state of the field-split crystal-field states. We recall that the $|\Gamma_7\rangle$ consists of mixtures of $J_z = |\pm 5/2\rangle$ and $J_z = |\mp 3/2\rangle$ states, the $|\Gamma_6\rangle$ of $J_z = |\pm 7/2\rangle$ and $J_z = |\mp 1/2\rangle$ states, and the quartet of two doublets, where one is $|\Gamma_6\rangle$ and one $|\Gamma_7\rangle$ like. In the presence of an applied field the state with the largest J_z forms the lowest Zeeman state, and in addition the largest J_z becomes stabilized; i.e., the contribution of the larger J_z increases due to the field. As a result, in the $|\Gamma_6\rangle$ and $|\Gamma_8\rangle$ crystal-field schemes the lowest Zeeman states are dominated by $J_z = |\pm 7/2\rangle$. Consequently they have very similar orbital shapes and cannot be distinguished with our form factor experiment. In the $|\Gamma_7\rangle$ scenario, however, the $J_z = |\pm 5/2\rangle$ dominates the lowest Zeeman state and its orbital looks very different, resulting in a reversed anisotropy of the form factor. Therefore, the observed form factor *anisotropy* can rule out the $|\Gamma_7\rangle$ as ground state. In contrast, neither in Ref. 2 nor in Ref. 4 is the anisotropy in the magnetization and/or susceptibility due to the crystal-field ground state shown or taken into account. However, without this information it is difficult to determine crystal-field ground states from magnetic measurements where thermal averaging, exchange, possible Kondo interactions, etc., alter the moments but are not easily taken care of.

A $|\Gamma_6\rangle$ ground state would be in agreement with the entropy findings of the specific heat,[2] but as has been pointed out in Sec. II B, it fails to explain the double-peak structure in the inelastic neutron scattering data. All inelastic neutron scattering data exhibit a double-peak structure at all temperatures and can be analyzed consistently with a $|\Gamma_8\rangle$ quartet ground state and two ground-state excitations. From the present experiment with 12 meV incident energy and from the previous one with 17 meV we can conclude further that there is no additional ground-state excitation within an energy window up to 15 meV.

However, it should be mentioned that additional peaks in the inelastic neutron data have been observed for example in $CeAl_2$.[23] Here strong electron phonon coupling gives rise to an additional peak in $S(Q,\omega)$. But this usually happens at higher energy transfers of acoustic zone boundary or optical phonon branches because the observation of such a bound state requires a certain phonon density of states which is not given in the range where acoustic branches rise steeply. For $CeAl_2$ the bound state is observed at 10 meV which coincides with the first peak in the phonon density of states. Ytterbium is not much heavier than cerium so that it is unlikely to have a flat phonon branch in the energy range of 3–4 meV. Hence we consider it unlikely that electron phonon coupling gives rise to an extra excitation.

We consider the quartet ground state in $YbInNi_4$ as the most likely solution. This makes us speculate whether $YbInNi_4$

is a candidate for quadrupolar order as in, e.g., CeB_6. The nature of the magnetic order in $YbInNi_4$ certainly deserves more investigation so that hopefully a better understanding of the apparent discrepancy of the entropy findings of R ln2 by Sarrao *et al.* and a $|\Gamma_8\rangle$ quartet ground state can be achieved.

IV. SUMMARY

The crystal-field scheme of $YbInNi_4$ has been determined with magnetic form factor and inelastic neutron scattering measurements. The asymmetry of the magnetic form factor clearly rules out a $|\Gamma_7\rangle$ doublet as ground state (see Fig. 2) and would be in line with either a $|\Gamma_6\rangle$ or $|\Gamma_8\rangle$ ground state. A quasiquartet ground state, where the two doublets are 1 meV apart, would not yield two almost equally strong excitations in the inelastic neutron data at 5 K since the first excited state would not be sufficiently populated (see Fig. 5). The inelastic neutron data confirm the existence of two crystal-field excitations at 3.2 and 4.4 meV at low temperatures and due to selection rules this is only possible for a $|\Gamma_8\rangle$ quartet ground state.

ACKNOWLEDGMENTS

We would like to thank Andrew Boothroyd for helpful discussions. T.W. is supported by the Bonn-Cologne Graduate School of Physics and Astronomy.

[1] I. Felner *et al.*, Phys. Rev. B **35**, 6956 (1987).
[2] J. L. Sarrao *et al.*, Phys. Rev. B **57**, 7785 (1998).
[3] A. Severing, E. Gratz, B. D. Rainford, and K. Yoshimura, Physica B **163**, 409 (1990).
[4] P. G. Pagliuso, J. D. Thompson, J. L. Sarrao, M. S. Sercheli, C. Rettori, G. B. Martins, Z. Fisk, and S. B. Oseroff, Phys. Rev. B **63**, 144430 (2001).
[5] I. Aviani, M. Ocko, D. Starescinic, K. Biljakovic, A. Loidl, J. Hemberger, and J. L. Sarrao, Phys. Rev. B **79**, 165112 (2009).
[6] K. W. H. Stevens, Proc. Phys. Soc. A **65**, 209 (1951).
[7] T. Mito, T. Koyama, M. Shimoide, S. Wada, T. Muramatsu, T. C. Kobayashi, and J. L. Sarrao, Phys. Rev. B **67**, 224409 (2003).
[8] T. Goto, E. V. Rozenfeld, K. Yoshimura, W. Zhang, M. Yamada, and H. Kageyama, J. Phys. Condens. Matter **15**, 2811 (2003).
[9] T. Mito, M. Nakamura, M. Otani, T. Koyama, S. Wada, M. Ishizuka, M. K. Forthaus, R. Lengsdorf, M. M. Abd-Elmeguid, and J. L. Sarrao, Phys. Rev. B **75**, 134401 (2007).
[10] R. J. Birgeneau, J. Phys. Chem. Sol. **33**, 59 (1972).
[11] T. Park, V. A. Sidorov, J. L. Sarrao, and J. D. Thompson, Phys. Rev. Lett. **96**, 046405 (2006).
[12] P. J. Brown, in *International Tables for Crystallography*, Vol. C, edited by A. J. C. Wilson (Reidel, Dordrecht, 1992), Chap. 4.4.5, pp. 391-399.
[13] J. X. Boucherle, F. Givord, S. Raymond, J. Schweizer, E. Lelievre-Berna, and G. Fillion, J. Phys. Condens. Matter B **13**, 10901 (2001).
[14] J. X. Boucherle and J. Schweizer, Physica B **130**, 337 (1985).
[15] M. Rotter and A. T. Boothroyd, Phys. Rev. B **79**, 140405 (2009).
[16] P. Wolfers, J. Appl. Crystallogr. **23**, 554 (1990).
[17] V. F. Sears, Neutron News **3**, 26 (1992).
[18] P. Becker and P. Coppens, Acta Crystallogr. A **30**, 129 (1974).
[19] M. Bonnet, A. Delapalme, P. Becker, and H. Fuess, Acta Crystallogr. A **32**, 945 (1976).
[20] J X. Boucherle and J. Schweizer, J. Magn. Magn. Mater. **24**, 308 (1981).
[21] J. Schweizer, in *Neutron Scattering from Magnetic Materials*, edited by T. Chatterji (Elsevier B. V., Amsterdam, 2006), p. 153.
[22] M. Rotter *et al.*, McPhase, a software package for calculation of the phase diagrams and magnetic properties of rare-earth systems (2002-2008), available at [http://www.mcphase.de].
[23] M. Loewenhaupt and P. Fulde, Adv. Phys. **34**, 589 (1985).